AGU100 ADVANCING EARTH AND SPACE SCIENCE

JGR

Journal of Geophysical Research: Atmospheres

RESEARCH ARTICLE
10.1029/2018JD028741

Key Points:
- LIS flashes consist of solitary groups and periods of near-continuous illumination that we denote *series*
- A small fraction groups/series significantly brighten the flash, and these radiant pulses can be counted to produce an optical multiplicity
- Optical multiplicities and interseries intervals are total lightning products that may result from any process with strong optical emission

Correspondence to:
M. Peterson,
michaeljp24@gmail.com

Citation:
Peterson, M., & Rudlosky, S. (2019). The time evolution of optical lightning flashes. *Journal of Geophysical Research: Atmospheres*, *124*, 333–349. https://doi.org/10.1029/2018JD028741

Received 30 MAR 2018
Accepted 1 DEC 2018
Accepted article online 10 DEC 2018
Published online 15 JAN 2019

The Time Evolution of Optical Lightning Flashes

Michael Peterson[1] **and Scott Rudlosky**[2]

[1]Earth System Science Interdisciplinary Center/Cooperative Institute for Climate and Satellites-Maryland, University of Maryland, College Park, MD, USA, [2]NESDIS, STAR, SCSB, College Park, MD, USA

Abstract The composition and time evolution of lightning are examined using the Lighting Imaging Sensor (LIS). Frame-by-frame optical lightning measurements are clustered into features whose radiant energy, horizontal footprint, and timing may be analyzed statistically. A LIS *series* feature is used to describe distinct periods of near continuous illumination that persists over multiple LIS frames. Series are integrated into the LIS clustering hierarchy between the group and flash level. An average series illuminates 40% of the flash footprint while accounting for 20% of the flash radiance, and just 1% of the flash duration. LIS flashes typically contain optical emissions that are exceptionally radiant and may persist over multiple frames. Series features cluster these bright optical pulses, allowing their number and time separation to be quantified in each flash. This optical multiplicity averages 1.7 for flashes with at least one particularly radiant group. Multigroup series most often occur early in the flash duration with 13% to 18% at first light. Series are typically separated by 100 ms or more in multiseries flashes. Bright series, by contrast, typically occur in rapid succession, with at most a few dozen milliseconds between them. Because series are optical features, they may result from any physical process that produces strong optical emissions. The statistics presented herein support the idea that series may originate from multiple physical processes.

Plain Language Summary Satellite lightning imagers record lightning flashes at 500 frames per second. We use the Lightning Imaging Sensor (LIS) on the Tropical Rainfall Measuring Mission (TRMM) satellite to describe the time-evolution of lightning from first light through the end of the flash. The radiant energy of the flash may appear as isolated flickers, or it may occur as a stream of nearly continuous illumination coming out of the top of the cloud. We organize these sustained optical pulses into features called "series" and examine their energy and timing in the flash. Flashes and series are comprised of mostly dim optical emissions, but a small number of pulses substantially increase the energy of the flash. These bright "groups" and the "bright series" that contain them describe physical lightning processes that produce large amounts of light. The frequency of bright series and the amount of time between subsequent bright series agree with ground-based measurements of return strokes and physical processes known as K-changes. Thus, lightning imagers may observe a combination of physical lightning processes.

1. Introduction

Lightning is detected from orbit by recording the transient flashes of light that escape the top of the cloud. Space-based lightning imagers include the Optical Transient Detector (OTD, Boccippio et al., 2000) on the MicroLab-1 satellite (1995–2000), the Lightning Imaging Sensor (LIS, Blakeslee, Christian, et al., 2014; Christian et al., 2000) on both the Tropical Rainfall Measuring Mission (TRMM) satellite (1997–2015) and the International Space Station (2017 up to present), and the Geostationary Lightning Mapper (GLM, Goodman et al., 2013) on the Geostationary Operational Environmental Satellite (GOES) R-series (GOES16, 2016–present; GOES17, 2018–present). These sensors observe total lightning intracloud (IC) flashes plus cloud-to-ground (CG) flashes—with a high detection efficiency. TRMM-LIS, for example, detected ~69% of flashes at noon to ~88% at night (Boccippio et al., 2002; Mach et al., 2007).

Optical lightning measurements provided by OTD, LIS, and GLM are sufficient for a range of Earth system applications. LIS and OTD flashes have been used to document the global distribution of total lightning (Albrecht et al., 2016; Cecil et al., 2014; Christian et al., 2003) and its diurnal cycle (Bailey et al., 2007; Blakeslee et al., 1999). When aircraft data are introduced to account for the Electrified Shower Clouds that do not produce lightning (Mach et al., 2010), the diurnal cycle in Universal Time compares well with the climatological daily variation in the fair-weather electric field known as the Carnegie curve (Blakeslee, Mach, et al., 2014; Mach et al., 2011). The TRMM-LIS data set is particularly useful because it contains

coincident measurements from the TRMM Microwave Imager, Precipitation Radar, and Visible and Infrared Scanner (Kummerow et al., 1998). These instruments tie lightning production to thunderstorm features and characterize the cloud medium that optical emissions from lightning interact with along their path to the imager. Data fusion among the TRMM instruments has resulted in many comparisons between lightning activity and parameters describing the precipitation structure and microphysics of the parent thunderstorm (Blyth et al., 2001; Cecil et al., 2005; Liu et al., 2011, 2012; Peterson & Liu, 2011, 2013; Prigent et al., 2005; Takayabu, 2006; Xu et al., 2010). Peterson et al. (2017a) and Peterson, Rudlosky, et al. (2017) additionally showed how clouds in the vicinity of LIS flashes influence the spatial distribution of optical energy from lightning.

Analyses of total flash rates and the location of lightning relative to the storm structure are useful, but the time and position coordinates of lightning flashes only represent a small fraction of the data generated by OTD, LIS, and GLM. Lightning imagers are staring instruments that map the evolution of flashes at 500 frames per second. They monitor the 777.4-nm oxygen emission line to detect lightning during the day and at night. The radiant energy in each pixel on the Charge-Coupled Device array during a single frame is compared against a dynamic threshold that represents the background radiance of the scene without lightning. Once a pixel exceeds the dynamic background, an *event* is triggered. Events are the basic elements that describe optical lightning signals in the lightning imager data.

Collections of events are grouped in space and time into features that capture lightning phenomena. Christian et al. (2000) describe the clustering process for LIS. Contiguous events in the same frame are clustered into *groups* that describe the optical signals in the 2-ms window. Individual flashes are distinguished by clustering groups that occur within a certain distance and time of one another according to a weighted Euclidean distance function (Mach et al., 2007). Thunderstorm *areas* are approximated using a similar weighted Euclidean distance technique based on the separation of *flash* features.

Group and event data from OTD, LIS, and GLM have been used to characterize the optical signals produced by lightning in order to infer the physical lightning processes responsible for them. Koshak (2010) proposed using the Maximum Group Area (MGA) metric as a possible discriminator between CG and IC flashes. Koshak (2011) and Koshak and Solakiewicz (2015) subsequently developed algorithms to compute the fractions of CG and IC flashes—known as the Z-ratio (Mackerras et al., 1998; Prentice & Mackerras, 1977)—for a large sample of optical lightning flashes based on statistical differences in MGA between CG and IC flashes. Bitzer (2017) additionally inferred continuing currents by detecting collections of sequential groups in the same flash.

Unlike LF/VLF radio-based lightning locating systems, lightning imagers do not preferentially detect CG strokes. Any flow of current whose optical energy escapes the cloud top in sufficient quantities to overcome the background threshold of the instrument will be detected. Peterson et al. (2017a) and Peterson, Rudlosky, et al. (2017), for example, used LIS data to map the lateral development of lightning flashes that propagate over substantial horizontal distances. Optical platforms provide additional insights into flash evolution and structure compared to the long-range networks with similar global-scale domains. They cannot, however, directly observe the polarity, altitude, CG versus IC classification, or the number of strokes (i.e., the multiplicity) in a given flash. Moreover, the optical signals may be modified by scattering in the surrounding cloud medium (Peterson et al., 2017a; Peterson, Rudlosky, et al., 2017) or variations in LIS sensitivity due to instrument performance (i.e., Charge-Coupled Device array pixel and quadrant, Zhang et al., 2018) and background radiance (Figure 3 in Peterson & Liu, 2013), even to the point of preventing detection entirely.

Identifying the physical process producing optical emissions from a signature in the optical data is complicated by not only interactions with the intervening cloud medium but also the host of light-producing phenomena in the Earth-atmosphere system. Temporarily setting aside all considerations for instrument sensitivity and scan geometry, processes that emit transient optical signals that may be recorded by an optical platform include strokes (Koshak, 2010), continuing current (Bitzer, 2017), *M* components (Flache et al., 2008), leader development, K-changes (Kitagawa & Brook, 1960; Thottappillil et al., 1990), K-process waves (Winn et al., 2011), transient luminous events such as jets (Su et al., 2003), and non-lightning phenomena such as glint, bolides (Borovička et al., 2017), and earthquake lights (Thériault et al., 2014). Many of these will rarely, if ever, contribute to the data records provided by current-generation lightning imagers. However, as there is an increasing focus on extracting information from the group

data and identifying physical lightning processes from the optical signatures they produce, it is necessary to consider what optical signals exist in the lightning imager data and how they may masquerade as a signature of a phenomenon of interest.

This study documents the time evolution of LIS flashes from first light through the end of the flash. Groups are organized into distinct optical pulses—denoted series in Peterson, Rudlosky, et al. (2017) and herein—to characterize the optical signals in a given flash. Series features describe periods of nearly continuous illumination separated by time periods with no detected optical emissions. General statistics are provided for LIS series features. Series are also used to determine at what points in time optical pulses occur in relation to the flash duration, how frequently they occur, and at what energies. The overall goal of this study is to provide a framework for intercomparing optical signals in the lightning imager data and a benchmark of expected results that will aid in developing optical signatures of physical lightning processes.

2. Data and Methodology

Optical lightning data are packaged in a hierarchical format that preserves the clustering relationships between events, groups, flashes, and areas. This study uses the science data set from TRMM-LIS (Blakeslee, 1998) to analyze the light curves produced by individual flashes. These data are available from the Global Hydrology Resource Center, one of the National Aeronautics and Space Administration's Distributed Active Archive Centers. The TRMM satellite operated for 17 years from December 1997 until April 2015. At a 34.9° inclination, TRMM-LIS provided coverage of the entire tropics. It observed the major lightning-producing *hot spots* of the world (Albrecht et al., 2016) including the southern United States, the Congo basin in Africa, Lake Maracaibo and the La Plata basin in South America, and India and the Maritime Continent in Asia. The TRMM domain notably excluded the northern Great Plains of North America as well as most of Europe and Central Asia. Though thunderstorms are common in these regions, they are not as prominent as the tropics in terms of global electrified weather (Peterson et al., 2017b).

2.1. Optical Lightning Groups and Series

The standard LIS science data set contains features that characterize optical signals in individual frames (groups and events) and for entire flashes. No standard LIS feature describes optical emissions on time scales in the intervening 2 orders of magnitude between 2 and 330 ms. Most flashes exhibit intermittent optical pulses separated by considerable periods of *darkness* (i.e., radiance below threshold and no recorded groups). Optical signals that persist over multiple frames such as the *time-adjacent groups* from Bitzer (2017) and flash propagation noted in Peterson et al. (2017a) and Peterson, Rudlosky, et al. (2017) are not well described in group and flash feature statistics.

The example LIS flash depicted in Figure 1 demonstrates the need for an intermediate optical lightning feature between the group and flash level. The flash occurred during TRMM orbit 15440 at 00:32:14 UTC on 8/3/2000. Figures 1a–1c and 1e–1g show LIS events (large boxes) and groups (small boxes) overlaid on TRMM Visible and Infrared Scanner channel 4 infrared brightness temperatures, and a time series of group footprint area (Figure 1d) and group (greyscale) and range of event (orange) radiance (Figure 1e) as a function of time since the beginning of the flash. Each of the panels depicts the progression of groups up to the specified group number. The panels show the group extent (color coded greyscale) compared to the unique flash footprint (dark gray) at that point in the flash duration. The most recent group center is colored yellow to distinguish it from previous groups with a similar color. The group times in each panel are noted in the time series (Figures 1d and 1e) with the panel letters drawn above the corresponding bars.

This flash occurred near the edge of the storm where light can escape the side of the cloud to illuminate the top of a lower cloud deck. This scenario is not uncommon with LIS and GLM observations, and scattering in the cloud medium can significantly modify the spatial radiance distributions for the most energetic groups. We have shown examples of this in Figure 1 of Peterson and Liu (2013), Figures 1 and 4 of Peterson et al. (2017a), and in Figures 3 and 4 of Peterson, Rudlosky, et al. (2017). Factors that affect the footprints (events) and lateral development (groups) of LIS flashes are discussed at length in Peterson et al. (2018), while this study focuses on the temporal evolution of optical LIS flashes.

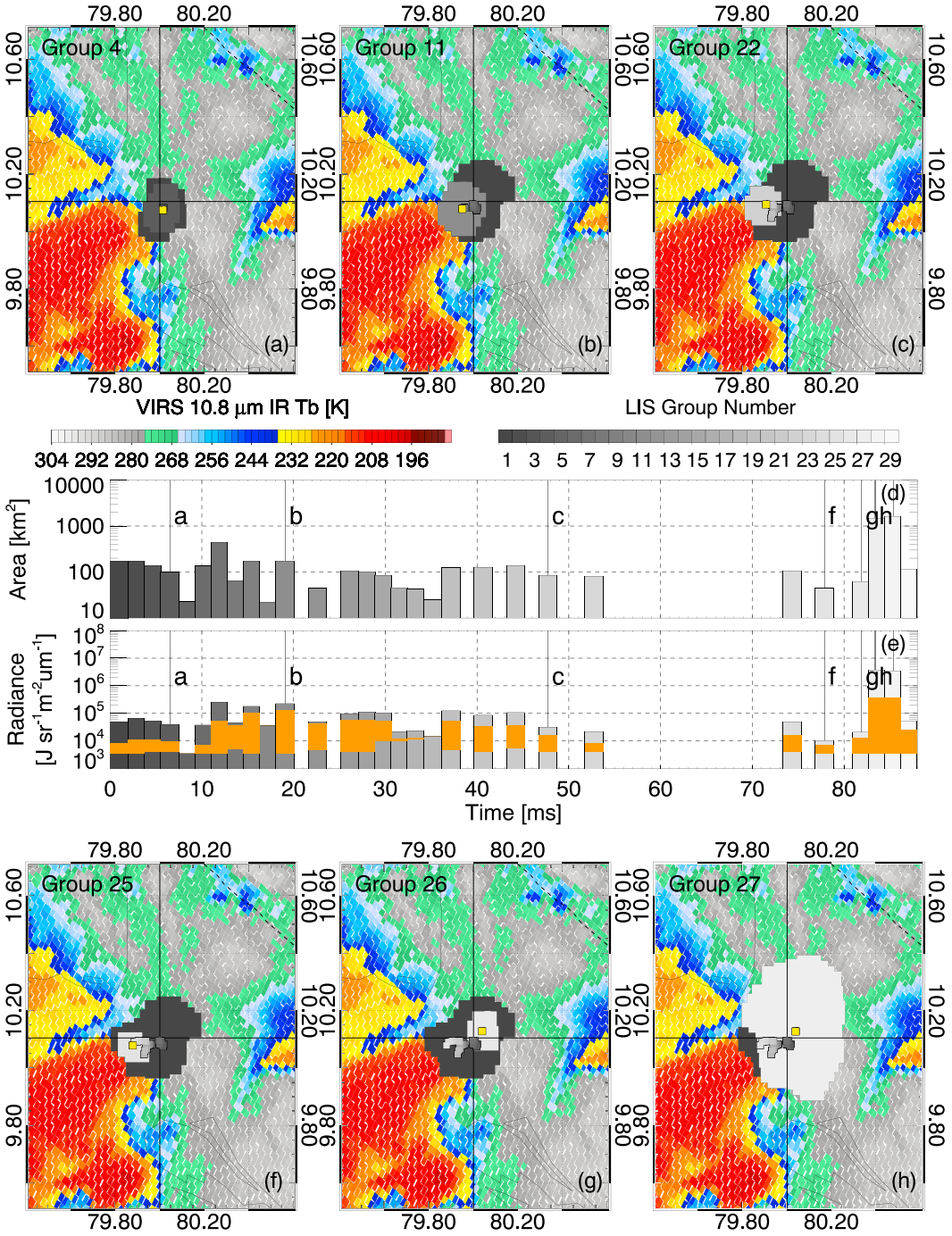

Figure 1. The evolution of the events (large pixels) and groups (small pixels) in a LIS flash detected on 3 August 2000 at 00:32:14 UTC (orbit 15440) and VIRS CH4 10.8-μm brightness temperatures. The progression of groups in the flash up to group 4 (a), 11 (b), 22 (c), 25 (f), 26 (g), and 27 (h) is shown along with the extent of the specified group relative to the overall flash footprint up to that point. A time series of group area is shown in Figure 1d and a time series of group (greyscale) and the range of event (orange) radiance is shown in Figure 1e. All LIS features are color coded to the same scale with the specified group in Figures 1a–1c and 1f–1h colored yellow. The center of the frame is aligned with the LIS flash centroid location. VIRS = Visible and Infrared Scanner; LIS = Lighting Imaging Sensor; VIRS = Visible and Infrared Scanner.

The flash in Figure 1 contains periods of both illumination and empty frames spread across its ~90-ms duration. Only 2 of 29 groups illuminated >1,000 km^2 and thus account for a significant fraction of overall flash footprint area. The flash illumination is not a random flickering. The cloud is constantly lit during the first

20 ms of the flash, while the groups progress increasingly westward from the group centroid location at first light. The next 30-ms interval continues this westward group motion with individual empty frames between groups. By Group 22 (Figure 1c), the groups in the flash have reached their maximum westward displacement. After one additional group, LIS detects no light for a period of 20 ms. Then, over the course of three groups, the optical emissions retrace the previous path from west to east, terminating with the MGA and continuous optical emission for four LIS frames (~8 ms).

This flash can be divided into two major periods of optical emission: the westward propagation during the first 54 ms of the flash, and the groups surrounding the MGA starting at 74 ms. The first period accounts for 24 of the 29 groups in the flash but less than half of its footprint area. The large number of groups in clusters like this bias the overall group-level statistics toward low-energy signals ($< 10^5$ J·sr^{-1}·m^{-2}·μm^{-1}) rather than toward the large bright pulses ($> 10^6$ J·sr^{-1}·m^{-2}·μm^{-1}) that may be associated with return strokes (i.e., Koshak, 2010) and luminous cloud discharges. The second period contains six groups that account for 80% of the total optical energy of the flash and illuminate a larger cloud area than the first 24 groups, combined. Thus, this type of highly radiant group can dominate the flash-level properties such as the footprint area, total radiance, and number of events.

Defining an optical lightning feature between the group and flash level in the clustering hierarchy allows for equal comparison between the two distinct periods of optical emission in Figure 1. As in Peterson, Rudlosky, et al. (2017), we construct a series feature to fill this role. A series is defined as any cluster of groups in the same flash where the groups occur in quasi-sequential frames. We use the term *quasi-sequential* to signify that groups can be separated by a small number of empty frames and still be considered part of the same series. This consideration is made because the group energy in many clusters borders the minimum threshold for detection. An example can be found in the first six groups of the flash in Figure 1 where the maximum energy of the brightest event in each group only reaches 1×10^4 J·sr^{-1}·m^{-2}·μm^{-1} compared to minimum detected event energy of 3×10^3 J·sr^{-1}·m^{-2}·μm^{-1} for the flash. The purpose of the series feature is to distinguish periods of optical emission that are clearly separated from one another. The existence of one or two empty frames interrupting an otherwise continuous period of optical emission does not fit the model of the series feature, as these frames could result from the optical signals momentarily falling below the dynamic threshold.

We examine the sensitivity of our series features to the chosen empty frame threshold by constructing a data set of two million LIS flashes that considers the three most elementary definitions of quasi-sequential groups. These definitions include no empty frames allowed between groups in the same series—which is identical to the time-adjacent groups in Bitzer (2017)—and either 1 frame or 2 frames allowed between groups. Table 1 compares the resulting statistics. The series statistics are divided between singleton (one group) series and multigroup series.

The key difference between series empty frame thresholds is the number of singleton series. Nearly 12 million singleton series are identified in our 2 million LIS flashes with the time-contiguous group case. Allowing single empty frames between groups in the same series reduces the number of singletons by 1.7 million as solitary groups are ingested into an additional 200,000 multigroup series. This can also be seen in the average series duration, which increases from 3.3 to 4.3 ms as the average group count reaches 3.

Allowing for a two-frame gap between groups in the same series further reduces the number of singleton series while increasing multigroup series durations and group counts. The fractions of propagating multigroup series also increase with the gap threshold from 5.3% to 5.9%, and the frequency of series lasting longer than 8 ms increases by ~6% per intervening empty frame allowed. The average series-related properties of flashes also change with the series definition. The number of singleton series per flash decreases with less restrictive series definitions (5.9 with no gap to 4.4 with a two-frame gap), while the flash-average fractions of groups in multigroup series and multigroup series fractions of the flash duration increase from 52% to 65% and 4.5% to 6.8%, respectively.

These variations provide evidence for a reorganization of singleton series into multigroup series as the threshold is relaxed. Many properties of multigroup series are relatively stable between the series definitions considered, however. The footprint sizes total radiances, and radiance ratios of LIS series features (singletons and

Table 1
Sensitivity of Series Definition to Maximum Allowed Gap Between LIS Frames

	Groups in consecutive frames		≤ 1 frame gap between groups		≤ 2 frame gap between groups	
	Singleton series	>1 groups	Singleton series	>1 groups	Singleton series	>1 groups
Series count	11,711,664	4,615,521	9,962,934	4,815,851	8,731,736	4,853,176
Fraction (%)	72	28	67	33	64	36
Series Mean						
Duration (ms)	-----	3.3	-----	4.3	-----	6.0
Group count	-----	2.7	-----	3.0	-----	3.3
Area (km^2)	90	180	91	182	91	185
Total radiance ($J{\cdot}sr^{-1}{\cdot}m^{-2}{\cdot}\mu m^{-1}$)	4.4×10^5	2.0×10^6	4.5×10^5	2.0×10^6	4.6×10^5	2.1×10^6
Radiance ratio	3.0	6.5	3.1	6.5	3.1	6.6
Series fraction (%)						
Propagating	-----	5.3	-----	5.7	-----	5.9
Duration > 8 ms	-----	5.6	-----	11	-----	18
Flash count	2,000,000	2,000,000	2,000,000	2,000,000	2,000,000	2,000,000
Flash mean						
Series count	5.9	2.3	5.0	2.4	4.4	2.4
Series percent of total groups	48	52	40	60	35	65
Series percent of total duration	-----	4.5	-----	5.6	-----	6.8

multigroup series) are nearly identical in all three definitions. The number of multigroup series that exist in the average LIS flash is also nearly constant at 2.4 for each case. Variations on the series definition affect the organization of relatively dim optical pulses and have less of an effect on sustained periods of illumination or intense optical pulses. We choose to employ the one-frame gap definition (2 ms) for the remainder of this study because it has the smallest temporal gap between quasi-sequential groups that still allows for the possibility of empty frames interrupting otherwise continuous periods of emission, as observed in Figure 1.

2.2. Optical Group and Series Database

A LIS database is constructed to describe the time evolution of the groups that comprise optical flashes. This database summarizes the properties of 20 million series features in 2.6 million flashes that were observed across the tropics between 1998 and 2000. Two years are sufficient to assemble a robust yet manageable sample for statistical comparisons. This time period occurred before the TRMM boost to a higher orbit in 2001. Moving from a 350-km altitude to a 400-km altitude increased the sizes of the LIS pixels. However, Cecil et al. (2014) suggest that this maneuver should not have a pronounced impact on LIS detection efficiency because flashes tend to be larger than individual events and the threshold settings were not changed postboost.

The database inserts series into the optical lightning clustering hierarchy between the flash and group levels such that series are children of flashes and groups are children of series. The footprint, duration, total radiance, and number of groups and events are reported for each series as they are for each flash in the standard science data set. The number of series for each flash and the total duration of all series also are added along with several derived parameters from Peterson et al. (2017a) and Peterson, Rudlosky, et al. (2017): the maximum separation of groups and events in each flash and series, and the maximum and minimum group and event radiances. As in Koshak (2010), we also compute the MGA and maximum number of events per group. Finally, for each flash, we calculate the average and standard deviation of the radiance of its constituent groups. We then count the number of groups that exceed one, two, or three standard deviations above the mean group radiance (i.e., 1-sigma, 2-sigma, or 3-sigma increases). Unlike the absolute energies of groups and flashes, these metrics identify periods of significant brightening above the baseline optical energy of the

flash that is usually dominated by the numerous relatively dim groups in a typical multigroup flash (i.e., Figure 1).

The new LIS database augments the standard LIS science data set (Blakeslee, 1998) by describing lightning in terms of flashes, distinct optical pulses (series), and individual frames (groups). LIS area and event features are not included. We preserve the addressing system from the LIS science data set to enable comparisons between the three feature levels in each LIS recording. The LIS series database may be easily reconstructed from the LIS science data using our above definitions of series and optical lightning metrics (section 2.1). We will also provide a copy of the database upon request.

The utility of the series database is shown with a second example LIS flash depicted in Figure 2. This flash occurred at 3:12:43 UTC on 27 February 1998 during TRMM orbit 1439. As with the first case, its 211 groups contain time periods with bright pulses (Figures 2a and 2f, Groups 1–24 and 187–208) and lateral flash development (Figures 2b, 2c, and 2f, Group 58–165). However, the series (shaded blue in Figures 2d and 2e) organize the flash into 11 multigroup clusters separating distinct periods of illumination. The longest of these periods lasted 90 ms. The MGA (1,100 km^2) and highest-radiance group (3.7×10^6 $J{\cdot}sr^{-1}{\cdot}m^{-2}{\cdot}\mu m^{-1}$) occurred in the first series lasting 45 ms where the groups remained relatively stationary with time (Figure 2a). The next nine series describe the lateral flash development (Figures 2b, 2c, and 2f). The final series contained a second bright pulse that produced a group whose radiance exceeded the 3-sigma threshold for the flash (Figure 2g). The last panel (Figure 2h) depicts the final flash footprint and overall progression of groups in the flash. Also note that there is an artifact in the event data of the flash in Figure 2 that produces a rectangular feature in the flash footprint. Flashes like this demonstrate that the group-level data we base our series on remain stable even when issues exist in the event-level data.

3. Results

The following sections document the statistical relationships between the elements that comprise optical LIS flashes. Section 3.1 compares the scale and optical characteristics of groups, series, and flashes. Section 3.2 then examines the groups and series in optical flashes to quantify the frequency of optical emissions and when they occur in the flash.

3.1. Optical Flash Composition

Figure 3 summarizes the footprint area, duration, and radiance of LIS features. For the first time, series statistics (red) are compared with groups (blue) and flashes (black). The typical group in Figure 3a is relatively small with most being confined to footprint areas <100 km^2 (~5 LIS pixels). LIS series and flashes, meanwhile, typically have footprints that cover hundreds of square kilometers with parent flashes ($\bar{x}$: 303 km^2, σ: 318 km^2) naturally larger than child series ($\bar{x}$: 116 km^2, σ: 112 km^2). Figure 3b shows series and flash duration distributions. Groups and single-group series that would have durations <2 ms are not shown. Four out of every five flashes occur on time scales ranging from 100 ms to 1 s. Single-group flashes, which would not contain multiple-group series, account for 8% of the total. Multiple-group series rarely last beyond tens of milliseconds. Since singletons are excluded, the most common series configurations are those that persist for 2 or 3 frames (70% of all multigroup series). Distributions of the group, series, and flash total radiance are shown in Figure 3c. As with flash area, groups are relatively dim ($\bar{x}$: 6×10^4 $J{\cdot}sr^{-1}{\cdot}m^{-2}{\cdot}\mu m^{-1}$, σ: $2 \times$ $J{\cdot}sr^{-1}{\cdot}m^{-2}{\cdot}\mu m^{-1}$) while flashes are more than an order of magnitude brighter ($\bar{x}$: 9×10^5 $J{\cdot}sr^{-1}{\cdot}m^{-2}{\cdot}\mu m^{-1}$, σ: $2x10^6$ $J{\cdot}sr^{-1}{\cdot}m^{-2}{\cdot}\mu m^{-1}$), and series fill the middle ground between the two. In either case, the average flash radiance is collocated with the tail of the group distribution, indicating that only the largest and brightest groups compare with the areal extent or radiant energy of a LIS flash.

The flashes in Figures 3a–3c as well as their constituent groups and series encompass the full diversity of optical signals recorded by LIS. Figures 3d–3f normalizes the series and group features by the overall footprint areas, durations, and radiances of the flashes they comprise. Groups and series can cover anywhere from 1% of the flash footprint to 100%, with the average series illuminating 40% of the overall footprint. Only the top 4% of series and top 3% of groups illuminate the entire flash footprint. Series that last the entire flash duration are less common than those that illuminate the full flash footprint (Figure 3e). Even the longest series in Peterson, Rudlosky, et al. (2017) contain time periods with empty frames lasting tens of milliseconds. The average LIS series spans <1% of the overall flash duration with most series (63%) lasting between

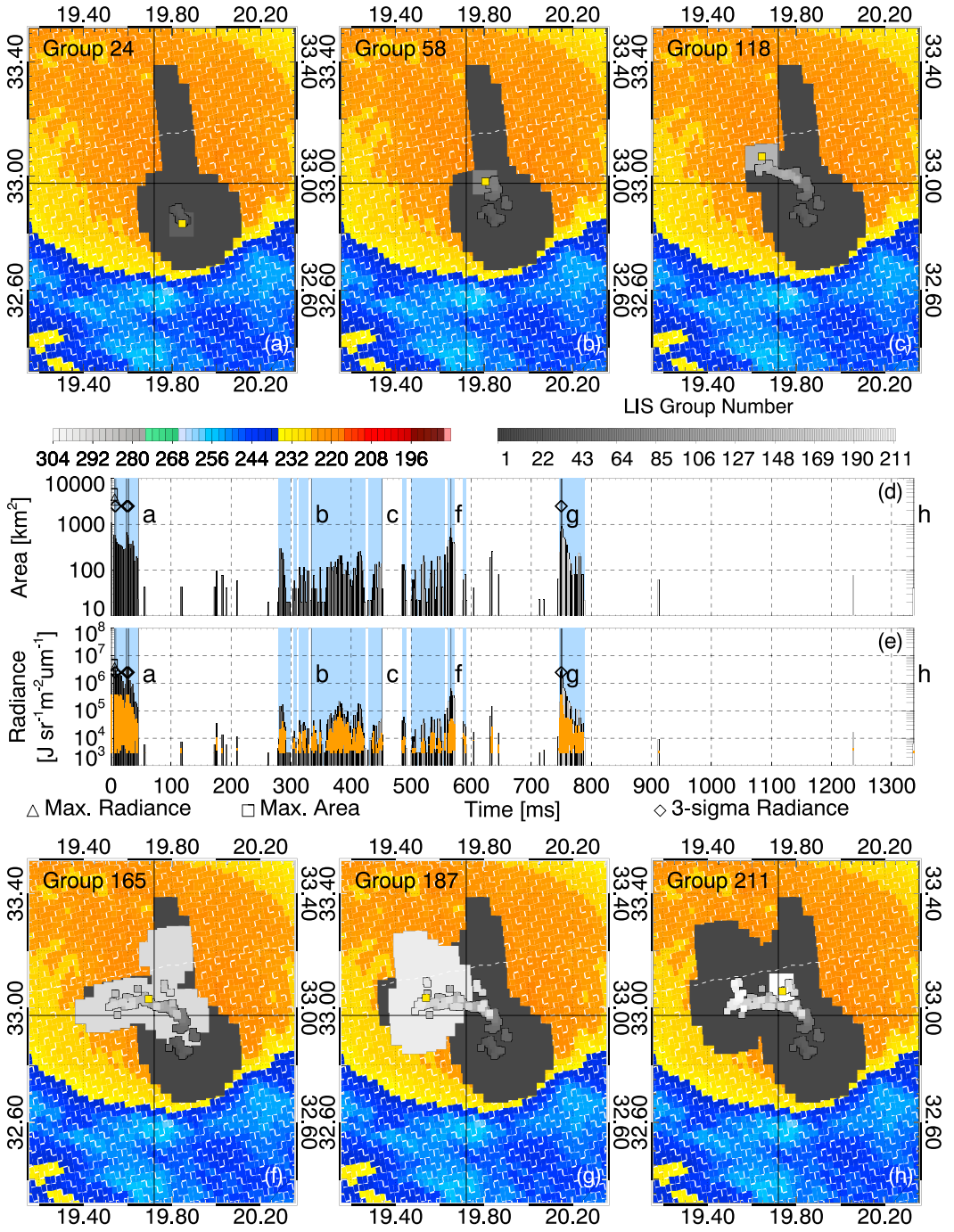

Figure 2. As in Figure 1 for another example LIS flash on 27 February 1998 at 03:12:43 UTC (orbit 1439) with 211 groups clustered into 11 multigroup series shaded blue in Figures 2d and 2e. LIS = Lighting Imaging Sensor.

0.1% and 1% of the flash duration. The remaining 99 + % are split between intermittent single-group pulses of light and empty LIS frames. In terms of flash-normalized radiance, most groups and series individually account for anywhere between 0.01% and 100% of the total flash energy. Series are more energetic than groups and generally have a higher fraction that account for virtually all of the optical energy in the flash.

Figure 4 compares the radiance of a given group to the remaining groups in the same flash to identify periods of flash brightening. Figure 4a shows the distribution of group radiance normalized by the mean group

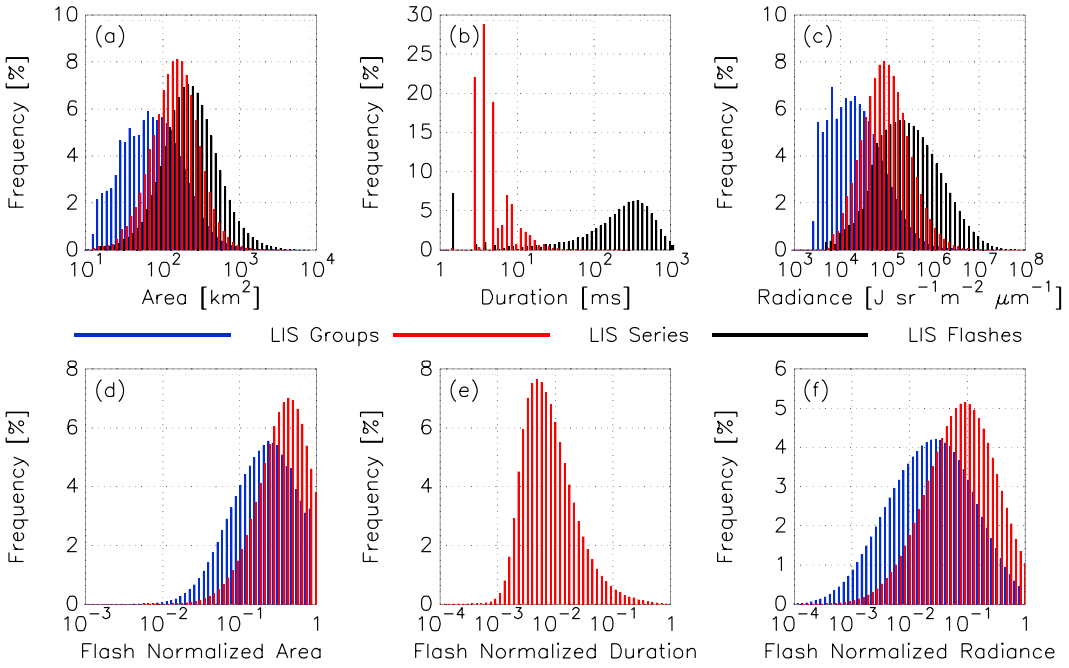

Figure 3. Distributions of the illuminated areas (a, d), durations (b, e), and total radiances (c, f) of LIS group, series, and flash features. The bottom row is presented as a fraction of the flash area (d), duration (e), and radiance (f). LIS = Lighting Imaging Sensor.

radiance for the flash. Normalized radiances are reported in relation to the flash mean ($\bar{x}$) group radiance and standard deviation (σ). A value of +1-sigma, for example, corresponds to one standard deviation above the mean. The distribution of group radiance (blue bars) is not a Gaussian distribution with a symmetrical bell curve around the mean. Instead, it consists of a high frequency of relatively dim groups offset by a small number of high-radiance groups. This is consistent with the example LIS flashes from Figures 1 and 2 where the majority of groups illuminated only a few pixels while a select few groups were bright enough to illuminate nearly the entire flash footprint at once.

Substantial differences in energy, frequency, and propensity for lateral motion—both herein and from Peterson et al. (2017a) and Peterson, Rudlosky, et al. (2017)—suggest that the multitude of low-energy groups have a different physical origin than the infrequent high-energy groups. The distribution in Figure 4a would then result from a superposition of the low-energy and high-energy histograms. The simplest method for distinguishing bright groups that result from high-current processes such as return strokes

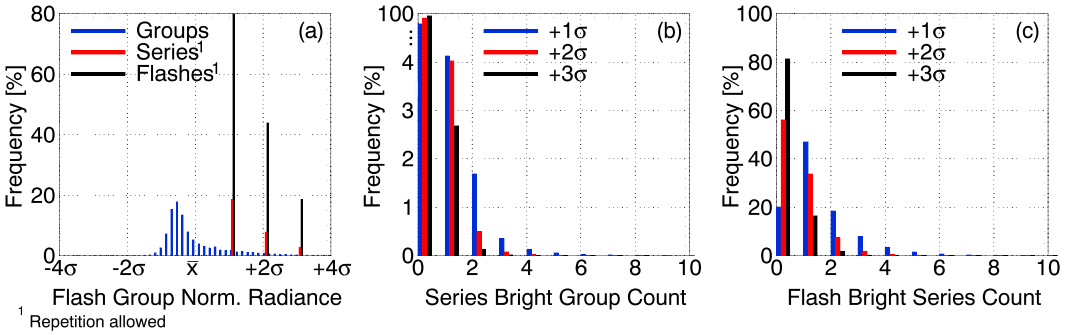

Figure 4. Distributions for the normalized radiance of groups in a flash (a), the number of bright groups per series (b), and the number of bright series per flash (c). Bright groups and series are defined at the +1σ, +2σ, or +3σ level with the frequencies in each case shown in Figure 4a.

(i.e., Koshak, 2010) from dim pulses that often trace large-scale leader development is to assign a constant threshold at the tail end of the distribution in Figure 4a. Any groups whose normalized energy lies above this threshold are considered a *bright group*. Figure 2 reported groups whose radiances reached the 3-sigma level for the flash (diamond symbols in Figure 2d). Figure 4a shows that the 3-sigma level accounts for the top percent of groups that are found in 3% of all series and 19% of all flashes. However, a lower threshold may be sufficient to isolate these bright groups and the series that contain them. A 2-sigma threshold accounts for the top 5% of all groups that occur in 8% of all series and 44% of flashes, and a 1-sigma threshold accounts for the top 13% of groups in 19% of all series and 80% of flashes. The chosen threshold determines the intensity of groups that will be identified with higher thresholds limited to only the most energetic groups.

Figure 4b shows the number of bright groups that are typically found in a single series for each sigma level. As in Figure 4a, most series do not contain a bright group. Moreover, the majority of bright series contain only one exceptionally radiant group at any sigma level. However, there is a small fraction of series that contain multiple radiant groups. The 1–2% of series contain two bright groups at the 1-sigma level, while fewer than 1% contain 3. Thus, when Bitzer (2017) discusses continuing current with five or more sequential groups, these are very rarely sequences of groups with a sustained high radiance—if they contain a bright group in the first place.

The key benefit of using series to examine high-radiance groups is that they quantify the number of bright groups and distinct optical pulses that contain such groups. While the MGA or maximum number of events per group identifies only the single most exceptional group in the flash, bright series can be used to define an optical multiplicity that counts the number of radiant pulses that were observed over the course of the flash. The optical multiplicity is a similar concept to the multiplicity reported by ground-based networks that count the energetic radio signals produced by individual distinct strokes. The optical multiplicity is more generalized, however, since it is based on optical observations of total lightning activity.

Though the radio-based multiplicity is not expected to generally match the optical multiplicity, the radio-based multiplicity statistics are well established and provide a point of reference for the optical multiplicity. The average radio-based multiplicity for a population of flashes has generally been reported between 1.2–1.7 (Yair et al., 2014), 2.1–2.4 (Rakov & Huffines, 2003), and 2.7 (Diendorfer et al., 1998). These values vary by region and can differ based on the detection efficiency of the lightning locating system and the flash clustering algorithm employed (Yair et al., 2014).

Figure 4c shows the distribution of optical multiplicity for LIS flashes. As in Figure 4a, 20% of flashes have no bright series at the 1-sigma level, 56% at the 2-sigma level, and 81% at the 3-sigma level. Another 47% of flashes for the 1-sigma level, 34% of flashes for the 2-sigma level, and 16% of flashes for the 3-sigma level contain exactly one bright series corresponding to a respective 59%, 77%, and 89% of the remaining flashes. The average optical multiplicity for LIS flashes is 1.4 for 1-sigma, 0.6 for 2-sigma, and 0.2 for 3-sigma. If flashes that produce a nearly constant radiance throughout their durations (i.e., with optical multiplicities of zero) are excluded, the average optical multiplicities become 1.7 for 1-sigma, 1.3 for 2-sigma, and 1.1 for 3-sigma. Thus, even though the optical multiplicity is likely to include signals from processes other than return strokes, the average number of radiant optical pulses in a flash generally agrees with the average number of powerful Radio Frequency (RF) pulses.

3.2. The Timing of Optical Pulses in LIS Flashes

Once groups that comprise distinct optical pulses are defined—bright or otherwise—we can examine when these pulses occur over the course of the flash. Figure 5 presents distributions of LIS series timing. Times are indicated as a fraction of the flash duration normalized to one. Figure 5a depicts the distributions of elongated and propagating series based on the definitions from Peterson et al. (2017a). Elongated series contain events that are separated by a longer distance than the characteristic diameter of the unique footprint area of the series. Propagating series similarly contain groups that are separated by a larger distance than the characteristic radius of the series footprint.

Elongated series are most common with the first (12%) and the final (3%) groups of the flash. Many of these are cases of flashes that consist of one or two groups. All other points within the flash duration are equally likely to contain an elongated series. Propagating series, by comparison, are most frequent toward the end of the flash. Aside from propagating series beginning at first light, the probability of series propagation

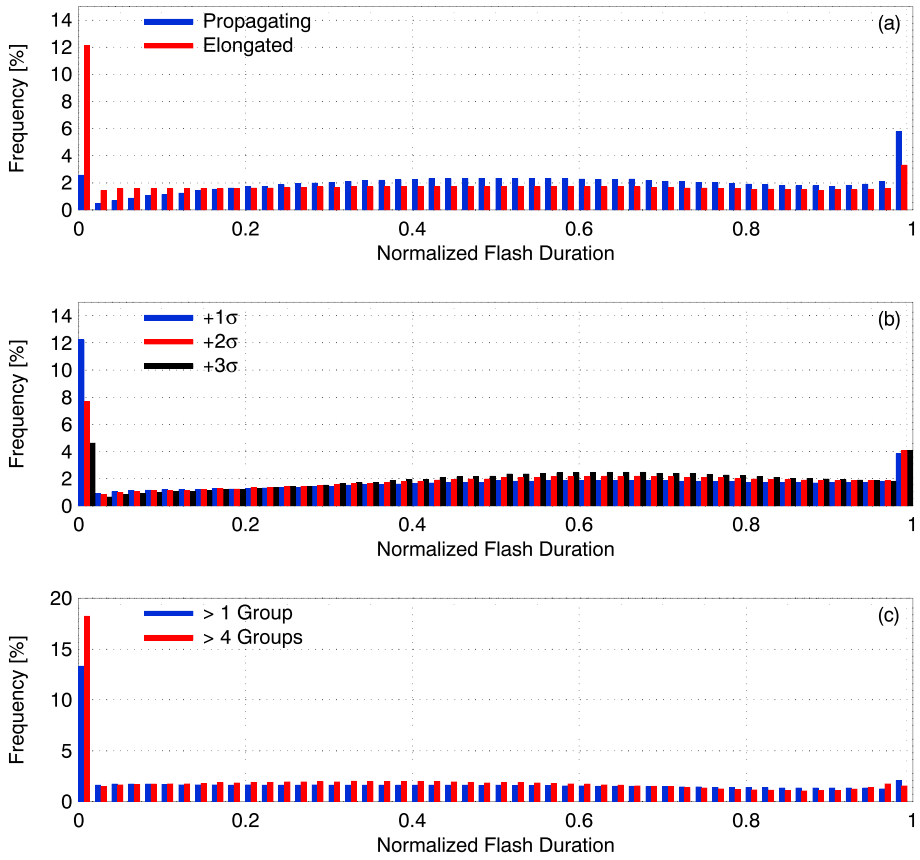

Figure 5. The frequency of propagating and elongated series (a), bright series (b), and multigroup series (c) as a function of the normalized time of occurrence in the flash duration (0: beginning, end: 1).

starts small and increases with time until approximately the flash midpoint. The most probable point in the flash to find a propagating series is at the very end, which accounts for 6% of the total.

Bright series emulate the behavior of both elongated and propagating series from Figure 5a. Figure 5b shows that bright series are most common with first light but otherwise infrequent in the initial frames of the flash. The bright series frequency increases until 60% of the flash duration. Bright series at the 1-sigma level are most concentrated in the first group of the flash, while 2-sigma and 3-sigma bright series are most likely to occur later in the flash between normalized times of 0.4 and 0.8. Bright series at each sigma level are nearly equally probable with the last group in the flash (4%).

Figure 5c shows distributions for the timing of series that persist for multiple groups. The general case of multigroup series is considered alongside series that contain five or more groups. Multigroup series are most likely early in the flash duration with 13% (2+ groups) to 18% (5+ groups) at first light. While the previous series categories become more common with time until the midpoint of the flash, the frequency of multigroup series decreases with time after 0.5. There is also a notable lack of a peak at the end of the flash.

The timing of series in relation to the most significant group in the flash can additionally be assessed. The left column of Figure 6 shows distributions for the timing of elongated and propagating series (Figure 6a), bright series (Figure 6c), and multigroup series (Figure 6e) relative to the series that contained the MGA. Positive time values indicate that the series occurred following the MGA while negative time values indicate the series occurred before the MGA. Elongated series (32%), bright series (45%–55%), and $>$4 group series (37%) are the most likely to contain the MGA (t = 0 ms). However, this is not always the case, and some series are observed more than 500 ms before or after the MGA series.

The remaining series are not distributed evenly around the MGA. Propagating series (Figure 6a) are more likely to occur after the MGA, while multigroup series (Figure 6e) are more frequent before the MGA. The

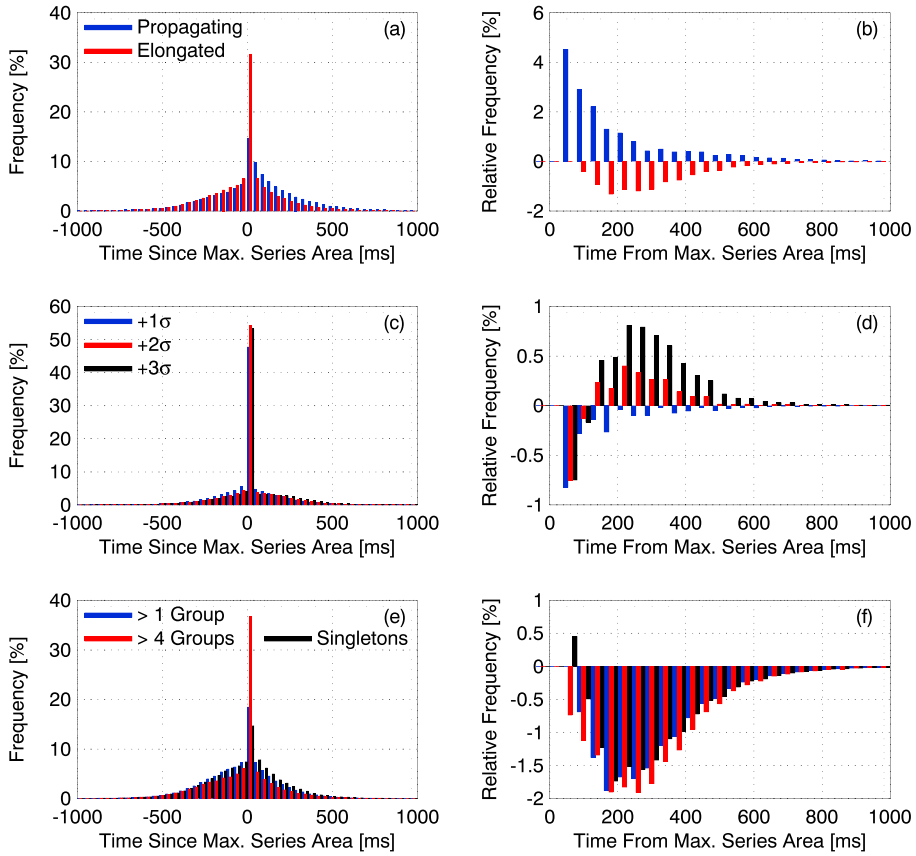

Figure 6. Distributions for the time difference between propagating or elongated series (a), bright series (c), and single or multigroup series (e) and the series that contains the MGA. The relative frequency between propagating or elongated series (b), bright series (d), and single or multigroup series (f) that occur after or before the MGA. MGA = Maximum Group Area.

right column in Figure 6 computes the difference in frequency between series that occur a certain length of time before the MGA and after the MGA. Positive values indicate a preference for series before the MGA and negative values indicate a preference for series following the MGA. Propagating series are more common after the MGA at all lengths of time depicted in Figure 6b. The strongest preference for propagation after the MGA can be found in the 40–80 ms range. Propagating series that occur at times longer removed from the MGA become less partial toward occurring after the MGA. In contrast to propagating series, elongated series are more common before the MGA for nearly all time intervals from the MGA. One key exception is the 40-ms period in the immediate vicinity of the MGA, where the relative frequency is approximately zero. The strongest preference for series before the MGA is found for time intervals removed from the MGA by 300 to 400 ms.

The relative frequency of bright series that occur before or after the MGA is not exclusively positive (i.e., always prefer following) or negative (i.e., always prefer preceding) as they were for propagating and elongated series. Bright series that occur within 100 ms of the MGA series are more likely to occur before the MGA than after the MGA at all three sigma levels. The relative frequency of bright series occurring beyond 100 ms from the MGA then depends on the sigma level. The relative frequency for 1-sigma bright series remains close to zero at all time periods with slightly negative values for most times. Bright series at the 2-sigma and 3-sigma levels, on the other hand, switch from negative to positive beyond 100 ms. With 1-sigma bright series, it is unclear which series contains the MGA. However, 2-sigma and 3-sigma series represent the most radiant pulses observed by LIS and usually coincide with the MGA. When a flash contains additional 2- or 3-sigma bright series that are separated from the MGA by a significant length of time (hundreds of milliseconds), then they tend to occur after the MGA as subsequent optical pulses following the largest group in the flash.

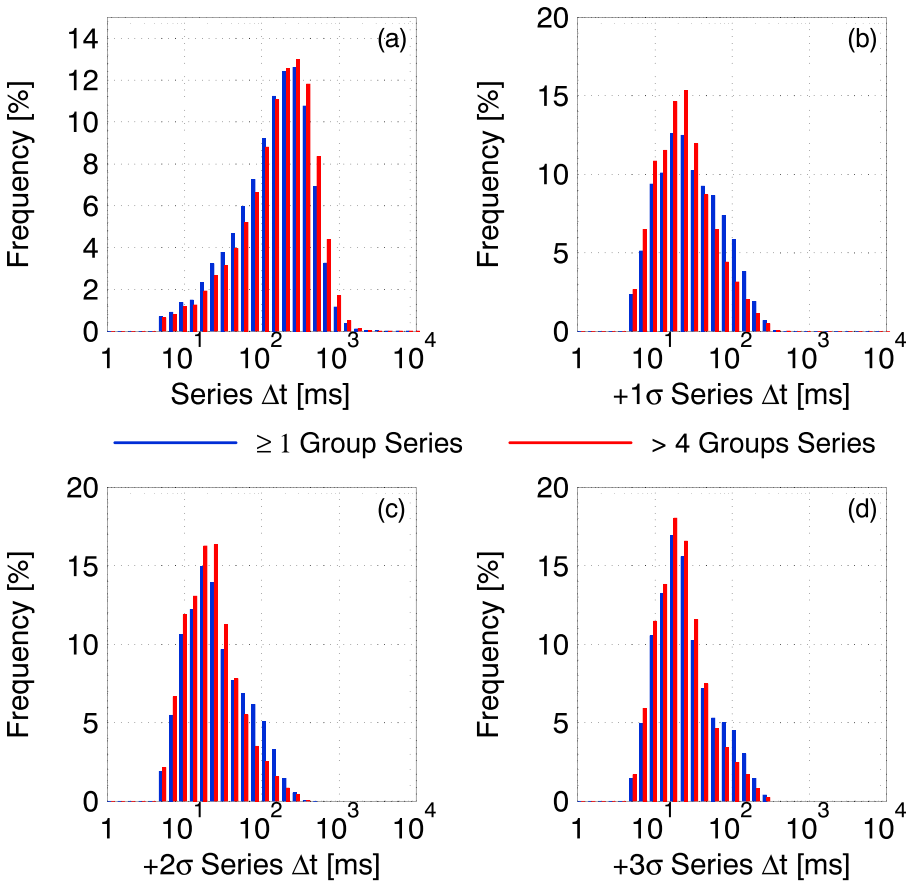

Figure 7. Distributions of the amount of time between all series (a) and bright series at the +1σ level (b), the +2σ level (c), or the +3σ level (d). Separate distributions are shown for series that contain >4 groups (red).

Figure 6f shows the relative frequency of singleton series, multigroup series, and series spanning more than four groups. Aside from one positive bar in the singleton series distribution, series production exclusively favors times before the MGA. This agrees with the timing of series where series frequencies were higher during early parts of the flash (Figure 5c) in contrast to the brightest and most significant groups that often occur later (Figure 5b).

The interseries interval characterizes the amount of time that passes from one distinct optical pulse to the next. The time interval between bright series is similar in concept to the interstroke interval discussed in the literature but for IC or CG processes that emit strongly at optical frequencies. Figure 7 shows interseries time interval distributions. Blue bars show the length of time between any two series in the flash, while red distributions only include series that contain >4 groups. In cases where more than one series is observed in a flash (Figure 7a), series are typically separated in time by 100 ms or more with a geometric mean of 144 ms (164 ms for series with >4 groups). Series may be separated by <10 ms or > 1 s. Limiting the analysis to only bright series reduces the mean interseries time interval by an order of magnitude. Figures 7b–7d show distributions for the time intervals between bright series at the 1-sigma (b), 2-sigma (c), and 3-sigma (d) level. In each case, multiple bright series in the same flash typically occur in rapid succession with at most a few dozen milliseconds between them. The geometric means for all multigroup bright series are 30 ms for 1-sigma, 27 ms for 2-sigma, and 26 ms for 3-sigma. Geometric means for series with >4 groups are slightly shorter at 25, 23, and 23 ms, respectively.

The ground-based RF measurements can help put these interseries intervals into perspective. Various studies have examined the time intervals between either strokes or K-changes. Estimated geometric means for interstroke intervals range from 40 to 70 ms (Rakov & Uman, 1990; Rakov et al., 1994; Thomson et al., 1984). K-changes, by comparison, occur at an increased cadence compared to strokes. Average values for the

interval between K-changes range from 8 to 13 ms (Kitagawa & Brook, 1960; Thottappillil et al., 1990). de Miranda et al. (2003), meanwhile, measured both K-change intervals and interstroke intervals and estimated geometric mean values of 12 and 69 ms, respectively, in line with the ranges from the previous studies. The spread in the interval times is likely influenced by the speed of K-waves in the lightning channel (Winn et al., 2011). At ~30 ms, the mean interseries interval sits between the average time intervals for strokes and K-changes. Because it is a total lightning quantity not limited to CG strokes, it likely encapsulates strokes, K-changes, and other optically radiant processes.

The literature additionally discusses the dependence of the interstroke interval on stroke order. The series data can be used to determine if the interval between bright series depends on the order of the pulse—first, second, third, etc. Figure 8 contains distributions for the interseries time intervals between the first and second bright series (Figure 8a), the second and third bright series (Figure 8b), the third and fourth bright series (Figure 8c), the and nth and nth + 1 bright series where $n > 3$ (Figure 8d) in the same flash. A 1-sigma threshold is used to identify multigroup bright series. Differences in the interval between bright series are most evident between the first and second and the second and third bright series. The distribution for the former has a geometric mean of 27 ms compared to 42 ms for the latter. The geometric mean increases to 49 ms for the interval between the third and fourth bright series and does not change appreciably for higher order bright series. Various studies have shown that order is irrelevant for interstroke time intervals (de Miranda et al., 2003; Thomson et al., 1984). For optical pulses, however, order does matter for the intervals between distinct radiant emissions.

4. Summary

This study examines lightning composition and time evolution using LIS imagery. A LIS *series* feature is used to describe distinct periods of near-continuous illumination that persist over multiple LIS frames. Optical flashes typically contain a few groups that are significantly more radiant than the remaining groups in the flash. Series features cluster these optical pulses, allowing the number and timing of radiant pulses in each flash to be analyzed.

The groups and series in a LIS flash can take on a wide array of optical characteristics. The largest and brightest of these compare with the optical energy and illuminated cloud area of the overall flash. However, these particularly radiant features only account for the top 4% of series and 3% of groups. Group footprint areas can account for as little as 1% or less of the overall flash area while series, on average, illuminate less than half (40%) of the optical flash area.

The typical LIS flash consists of mostly low-energy groups interspersed with the occasional high-radiance group. The difference in optical energy between the average LIS group and a bright group is considerable. For the flash in Figure 1, the bright groups in the series at the end of the flash illuminate a larger cloud area than the sum of the footprints of the preceding 24 groups combined. Differences can be noted in energy, timing, and behavior (i.e., stationary or propagating) between typical series and series that contain these bright groups. Bright series typically only contain one exceptionally radiant group, but some ($< 2\%$) contain multiple. Thus, bright series with five or more sequential groups do not typically describe a sustained period of high-radiance illumination but rather one to two bright groups with the remaining groups in the series less energetic.

We use bright series to define an optical multiplicity for LIS flashes that counts the number of bright series in a flash. While Koshak (2010) characterizes flashes based on their single most exceptional group, the optical multiplicity quantifies the number of radiant pulses that occur over the course of the flash duration. As an optical total lightning metric, these pulses may or may not result from strokes. Any physical process that produces a large amount of optical energy can create a bright series and advance the optical multiplicity. If flashes with at least one bright series are considered (i.e., not flashes whose optical energy remains nearly constant from one group to the next), the average optical multiplicities are between 1.7 (using a 1-sigma energy threshold) and 1.1 (using a 3-sigma energy threshold). Despite describing total lightning activity, these values generally agree with the radio-based multiplicity values in the literature.

The series cluster data are useful for comparing the characteristics of different optical pulses. We use series to produce statistics of when optical pulses occur in the flash duration. Elongated series are most common with

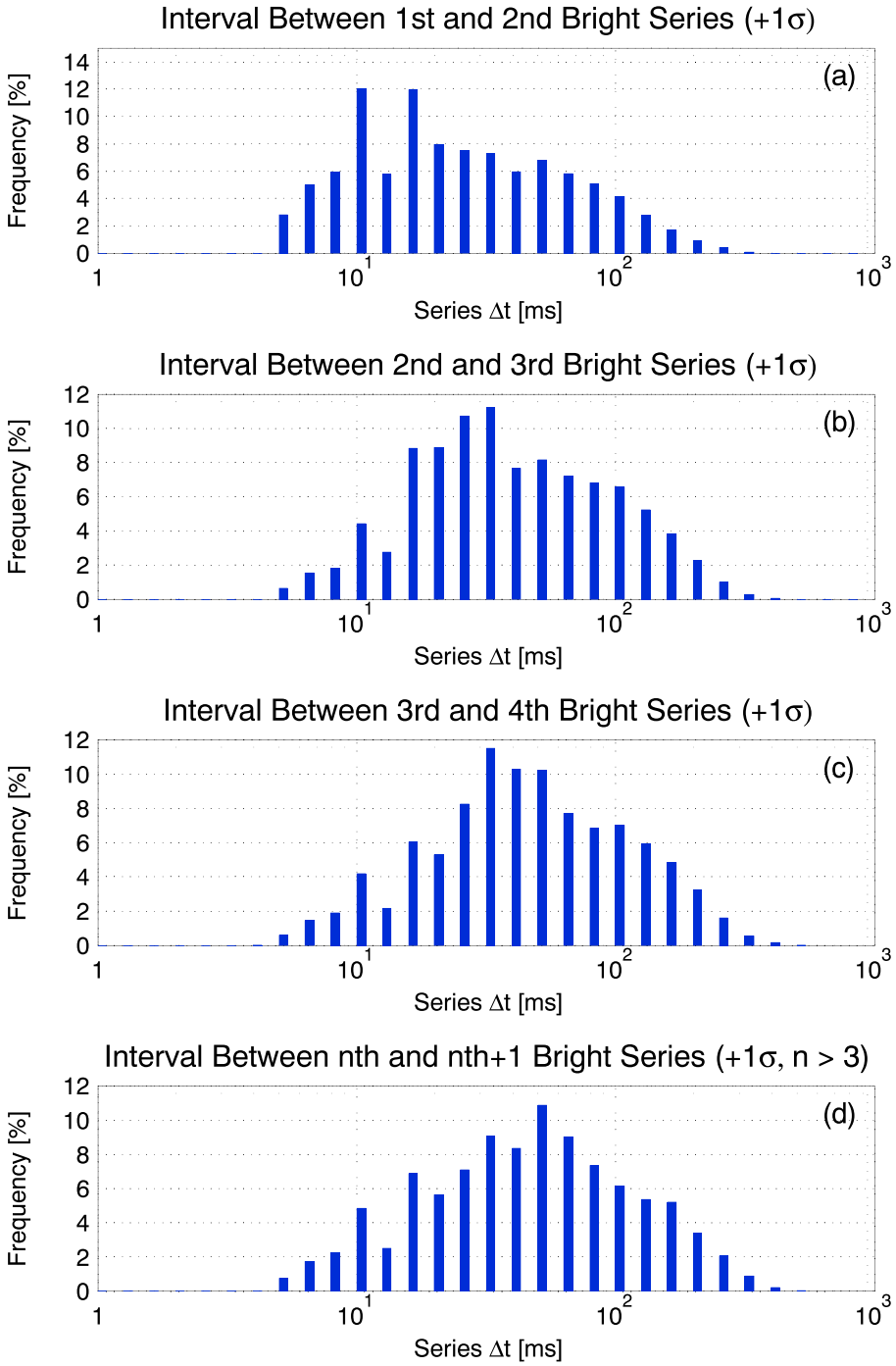

Figure 8. Distributions of the amount of time between the first and second bright series in a flash (a), the second and third bright series in a flash (b), the third and fourth bright series in a flash (c), and the *n*th and *n*th + 1 bright series in a flash with $n > 3$ (d).

the first group of the flash (12%) and the last group of the flash (3%). All other points within the flash duration are equally likely to contain an elongated series. Propagating series, by comparison, are most frequent toward the end of the flash. Aside from propagating series at first light, the probability of series propagation starts small and increases nearly fivefold by the flash midpoint. Bright series at the 1-sigma level are most concentrated in the first group of the flash while 2-sigma and 3-sigma bright series are most likely to occur later in the flash between 40% and 80% of the flash duration. Bright series that occur

with the last group in the flash are nearly equally probable at each sigma level (4%). Multigroup series are most likely to occur early in the flash duration, with 13% (2+ groups) to 18% (5+ groups) at first light.

The timing of series in relation to the most significant group of the flash is also assessed. Elongated series (32%), bright series (45–55%), and > 4 group series (37%) are the most likely to contain the MGA. Propagating series are more likely to occur after the MGA while multigroup series are more frequent before the MGA. The strongest preference for propagation after the MGA can be found in the 40- to 80-ms range. With 1-sigma bright series, it is unclear which series contains the MGA. However, 2-sigma and 3-sigma series represent the most radiant pulses observed by LIS and usually coincide with the MGA. When a flash contains additional 2- or 3-sigma bright series that are separated from the MGA by a significant length of time (hundreds of milliseconds), they tend to occur as subsequent optical pulses.

In cases where more than one series are observed in a flash, series are typically separated in time by 100 ms or more with a geometric mean of 144 ms (164 ms for series with >4 groups). Limiting analysis to just bright series reduces the mean interseries time interval by an order of magnitude. Multiple bright series in the same flash typically occur in rapid succession with at most a few dozen milliseconds between them. The time average interval between bright series (23–30 ms) falls between the geometric means for K-changes and strokes, adding weight to the idea that the optical multiplicity captures more than one physical lightning process. The order also matters for the interseries time interval, with the average increasing from 27 ms between the first and second bright series to 42 ms between the second and third bright series.

This study has provided an in-depth analysis of the temporal evolution of optical lightning flashes measured from orbit. Future work will leverage these insights into the composition of optical flashes and fusion with RF and ground-based electric field observations to investigate the optical signals produce by distinct types of physical lightning processes. This analysis will bolster the role of satellite optical platforms in characterizing lightning physics on global-scale domains.

Acknowledgments
This study was supported by NOAA grant NA14NES4320003 (Cooperative Institute for Climate and Satellites, CICS) at the University of Maryland/ESSIC and by NASA grant NNX17AH63G. The LIS science data set (Blakeslee, 1998) is available online from the NASA Global Hydrology Resource Center DAAC, Huntsville, Alabama, USA, one of NASA's Distributed Active Archive Centers (DAACs). The contents of this paper are solely the opinions of the authors and do not constitute a statement of policy, decision, or position on behalf of NOAA or the U.S. government.

References

Albrecht, R. I., Goodman, S. J., Buechler, D. E., Blakeslee, R. J., & Christian, H. J. (2016). Where are the lightning hotspots on Earth? *Bulletin of the American Meteorological Society*, *97*(11), 2051–2068. https://doi.org/10.1175/BAMS-D-14-00193.1

Bailey, J. C., Blakeslee, R. J., Buechler, D. E., & Christian, H. J. (2007). Diurnal lightning distributions as observed by the Optical Transient Detector (OTD) and the Lightning Imaging Sensor (LIS). *13th International Conference on Atmospheric Electricity, Int. Comm. on Atmos. Electr.* Beijing.

Bitzer, P. M. (2017). Global distribution and properties of continuing current in lightning. *Journal of Geophysical Research: Atmospheres*, *122*, 1033–1041. https://doi.org/10.1002/2016JD025532

Blakeslee, R. J., Christian, H. J., Stewart, M. F., Mach, D. M., Bateman, M., Walker, T. D., et al. (2014). Lightning Imaging Sensor (LIS) for the International Space Station (ISS): Mission description and science goals. In *XV Int. Conf. Atmos. Electricity* (15 pp.). Norman, OK.

Blakeslee, R. J., Driscoll, K. T., Buechler, D. E., Boccippio, D. J., Boeck, W. J., Christian, H. J., et al. (1999). Diurnal lightning distribution as observed by the Optical Transient Detector (OTD). In *11th International Conference on Atmospheric Electricity, NASA Conf. Publ., NASA/CP-1999–209261* (pp. 742–745).

Blakeslee, R. J., Mach, D. M., Bateman, M. G., & Bailey, J. C. (2014). Seasonal variations in the lightning diurnal cycle and implications for the global electric circuit. *Atmospheric Research*, *135-136*, 228–243. https://doi.org/10.1016/j.atmosres.2012.09.023

Blakeslee, R. J. (1998). Lightning Imaging Sensor (LIS) on TRMM science data. Dataset available online from the NASA global hydrology center DAAC. Huntsville, AL. https://doi.org/10.5067/LIS/LIS/DATA201

Blyth, A. M., Christian, H. J. Jr., Driscoll, K., Gadian, A. M., & Latham, J. (2001). Determination of ice precipitation rates and thunderstorm anvil ice contents from satellite observations of lightning. *Journal Atmospheric Research*, *59-60*, 217–229. https://doi.org/10.1016/S0169-8095(01)00117-X

Boccippio, D. J., Koshak, W., Blakeslee, R., Driscoll, K., Mach, D., Buechler, D., et al. (2000). The Optical Transient Detector (OTD): Instrument characteristics and cross-sensor validation. *Journal of Atmospheric and Oceanic Technology*, *17*(4), 441–458. https://doi.org/10.1175/1520-0426(2000)017<0441:TOTDOI>2.0.CO;2

Boccippio, D. J., Koshak, W. J., & Blakeslee, R. J. (2002). Performance assessment of the optical transient detector and lightning imaging sensor. Part I: Predicted diurnal variability. *Journal of Atmospheric and Oceanic Technology*, *19*(9), 1318–1332. https://doi.org/10.1175/1520-0426(2002)019<1318:PAOTOT>2.0.CO;2

Borovička, J., Spurný, P., Grigore, V. I., & Svoreň, J. (2017). The January 7, 2015, superbolide over Romania and structural diversity of meter-sized asteroids. *Planetary and Space Science*, *143*, 147–158. https://doi.org/10.1016/j.pss.2017.02.006

Cecil, D. J., Buechler, D. E., & Blakeslee, R. J. (2014). Gridded lightning climatology from TRMM-LIS and OTD: Dataset description. *Atmospheric Research*, *135-136*, 404–414.

Cecil, D. J., Goodman, S. J., Boccippio, D. J., Zipser, E. J., & Nesbitt, S. W. (2005). Three years of TRMM precipitation features. Part I: Radar, radiometric, and lightning characteristics. *Monthly Weather Review*, *133*(3), 543–566. https://doi.org/10.1175/MWR-2876.1

Christian, H. J., Blakeslee, R. J., Boccippio, D. J., Boeck, W. L., Buechler, D. E., Driscoll, K. T., et al. (2003). Global frequency and distribution of lightning as observed from space by the optical transient detector. *Journal of Geophysical Research*, *108*(D1), 4005. https://doi.org/10.1029/2002JD002347

Christian, H. J., Blakeslee, R. J., Goodman, S. J., & Mach, D. M. (Eds.) (2000). Algorithm Theoretical Basis Document (ATBD) for the Lightning Imaging Sensor (LIS), NASA/Marshall Space Flight Center, Alabama. Retrieved from http://eospso.gsfc.nasa.gov/atbd/listables.html, posted 1 Feb. 2000.

de Miranda, F. J., Pinto, O. Jr., & Saba, M. M. F. (2003). A study of the time interval between return strokes and K-changes of negative cloud-to-ground lightning flashes in Brazil. *Journal of Atmospheric and Solar - Terrestrial Physics*, *65*(3), 293–297. https://doi.org/10.1016/S1364-6826(02)00313-9

Diendorfer, G., Schultz, W., & Rakov, V. A. (1998). Lightning characteristics based on data from the Austrian lightning locating system. *IEEE Transactions on Electromagnetic Compatibility*, *40*(4), 452–464. https://doi.org/10.1109/15.736206

Flache, D., Rakov, V. A., Heidler, F., Zischank, W., & Thottappillil, R. (2008). Initial-stage pulses in upward lightning: Leader/return stroke versus M-component mode of charge transfer to ground. *Geophysical Research Letters*, *35*, L13812. https://doi.org/10.1029/2008GL034148

Goodman, S. J., Blakeslee, R. J., Koshak, W. J., Mach, D., Bailey, J., Buechler, D., et al. (2013). The GOES-R geostationary lightning mapper (GLM). *Journal Atmospheric Research*, *125-126*, 34–49. https://doi.org/10.1016/j.atmosres.2013.01.006

Kitagawa, N., & Brook, M. (1960). A comparison of intracloud and cloud-to-ground lightning discharges. *Journal of Geophysical Research*, *65*, 1189–1201. https://doi.org/10.1029/JZ065i004p01189

Koshak, W. J. (2010). Optical characteristics of OTD flashes and the implications for flash-type discrimination. *Journal of Atmospheric and Oceanic Technology*, *27*(11), 1822–1838. https://doi.org/10.1175/2010JTECHA1405.1

Koshak, W. J. (2011). A mixed exponential distribution model for retrieving ground flash fraction from satellite lightning imager data. *Journal of Atmospheric and Oceanic Technology*, *28*(4), 475–492. https://doi.org/10.1175/2010JTECHA1438.1

Koshak, W. J., & Solakiewicz, R. J. (2015). A method for retrieving the ground flash fraction and flash type from satellite lightning mapper observations. *Journal of Atmospheric and Oceanic Technology*, *32*(1), 79–96. https://doi.org/10.1175/JTECH-D-14-00085.1

Kummerow, C., Barnes, W., Kozu, T., Shiue, J., & Simpson, J. (1998). The Tropical Rainfall Measuring Mission (TRMM) sensor package. *Journal of Atmospheric and Oceanic Technology*, *15*(3), 809–817. https://doi.org/10.1175/1520-0426(1998)015<0809:TTRMMT>2.0.CO;2

Liu, C., Cecil, D., & Zipser, E. J. (2011). Relationships between lightning flash rates and passive microwave brightness temperatures at 85 and 37 GHz over the tropics and subtropics. *Journal of Geophysical Research*, *116*, D23108. https://doi.org/10.1029/2011JD016463

Liu, C., Cecil, D., & Zipser, E. J. (2012). Relationships between lightning flash rates and radar reflectivity vertical structures in thunderstorms over the tropics and subtropics. *Journal of Geophysical Research*, *117*, D06212. https://doi.org/10.1029/2011JD017123

Mach, D. M., Blakeslee, R. J., & Bateman, M. G. (2011). Global electric circuit implications of combined aircraft storm electric current measurements and satellite-based diurnal lightning statistics. *Journal of Geophysical Research*, *116*, D05201. https://doi.org/10.1029/2010JD014462

Mach, D. M., Blakeslee, R. J., Bateman, M. G., & Bailey, J. C. (2010). Comparisons of total currents based on storm location, polarity, and flash rates derived from high-altitude aircraft overflights. *Journal of Geophysical Research*, *115*, D03201. https://doi.org/10.1029/2009JD012240

Mach, D. M., Christian, H. J., Blackeslee, R. J., Boccippio, D. J., Goodman, S. J., & Boeck, W. L. (2007). Performance assessment of the optical transient detector and lightning imaging sensor. *Journal of Geophysical Research*, *112*, D09210. https://doi.org/10.1029/2006JD007787

Mackerras, D., Darveniza, M., Orville, R. E., Williams, E. R., & Goodman, S. J. (1998). Global lightning: Total, cloud and ground flash estimates. *Journal of Geophysical Research*, *103*, 19,791–19,809. https://doi.org/10.1029/98JD01461

Peterson, M., Deierling, W., Liu, C., Mach, D., & Kalb, C. (2017b). A TRMM/GPM retrieval of the total mean generator current for the global electric circuit. *Journal of Geophysical Research: Atmospheres*, *122*, 10,025–10,049. https://doi.org/10.1002/2016JD026336

Peterson, M., Rudlosky, S., & Deierling, W. (2018). Mapping the lateral development of lightning flashes from orbit. *Journal of Geophysical Research: Atmospheres*, *123*, 9674–9687. https://doi.org/10.1029/2018JD028583

Peterson, M. J., Deierling, W., Liu, C., Mach, D., & Kalb, C. (2017a). The properties of optical lightning flashes and the clouds they illuminate. *Journal of Geophysical Research: Atmospheres*, *122*, 423–442. https://doi.org/10.1002/2016JD025312

Peterson, M. J., & Liu, C. (2011). Global statistics of lightning in anvil and stratiform regions over the tropics and subtropics observed by TRMM. *Journal of Geophysical Research*, *116*, D23201. https://doi.org/10.1029/2011JD015908

Peterson, M. J., & Liu, C. (2013). Characteristics of lightning flashes with exceptional illuminated areas, durations, and optical powers and surrounding storm properties in the tropics and inner subtropics. *Journal of Geophysical Research: Atmospheres*, *118*, 11,727–11,740. https://doi.org/10.1002/jgrd.50715

Peterson, M. J., Rudlosky, S., & Deierling, W. (2017). The evolution and structure of extreme optical lightning flashes. *Journal of Geophysical Research: Atmospheres*, *122*, 13,370–13,386. https://doi.org/10.1002/2017JD026855

Prentice, S. A., & Mackerras, D. (1977). The ratio of cloud to cloud-ground lightning flashes in thunderstorms. *Journal of Applied Meteorology*, *16*(5), 545–550. https://doi.org/10.1175/1520-0450(1977)016<0545:TROCTC>2.0.CO;2

Prigent, C., Defer, E., Pardo, J. R., Pearl, C., Rossow, W. B., & Pinty, J.-P. (2005). Relations of polarized scattering signatures observed by the TRMM microwave instrument with electrical processes in cloud systems. *Geophysical Research Letters*, *32*, L04810. https://doi.org/10.1029/2004GL022225

Rakov, V. A., & Huffines, G. R. (2003). Return stroke multiplicity of negative cloud-to-ground lightning flashes. *Journal of Applied Meteorology*, *42*(10), 1455–1462. https://doi.org/10.1175/1520-0450(2003)042<1455:RMONCL>2.0.CO;2

Rakov, V. A., & Uman, M. A. (1990). Some properties of negative cloud-to-ground lightning flashes versus stroke order. *Journal of Geophysical Research*, *95*, 5447–5453. https://doi.org/10.1029/JD095iD05p05447

Rakov, V. A., Uman, M. A., & Thottappillil, R. (1994). Review of lightning properties from electric field and TV observations. *Journal of Geophysical Research*, *99*, 10,745–10,750. https://doi.org/10.1029/93JD01205

Su, H. T., Hsu, R. R., Chen, A. B., Wang, Y. C., Hsiao, W. S., Lai, W. C., et al. (2003). Gigantic jets between a thundercloud and the ionosphere. *Nature*, *423*(6943), 974–976. https://doi.org/10.1038/nature01759

Takayabu, Y. N. (2006). Rain-yield per flash calculated from TRMM PR and LIS data and its relationship to the contribution of tall convective rain. *Geophysical Research Letters*, *33*, L18705. https://doi.org/10.1029/2006GL027531

Thériault, R., St-Laurent, F., Freund, F. T., & Derr, J. S. (2014). Prevalence of earthquake lights associated with rift environments. *Seismological Research Letters*, *85*(1), 159–178. https://doi.org/10.1785/0220130059

Thomson, E. M., Galib, M. A., Uman, M. A., Beasley, W. H., & Master, M. J. (1984). Some features of stroke occurrence in Florida lightning flashes. *Journal of Geophysical Research*, *89*, 4910–4916. https://doi.org/10.1029/JD089iD03p04910

Thottappillil, R., Rakov, V. A., & Uman, M. A. (1990). K and M changes in close lightning ground flashes in Florida. *Journal of Geophysical Research*, *95*, 18,631–18,640. https://doi.org/10.1029/JD095iD11p18631

Winn, W. P., Aulich, G. D., Hunyady, S. J., Eack, K. B., Edens, H. E., Krehbiel, P. R., et al. (2011). Lightning leader stepping, K changes, and other observations near an intracloud flash. *Journal of Geophysical Research*, *116*, D23115. https://doi.org/10.1029/2011JD015998

Xu, W., Zipser, E., Liu, C., & Jiang, H. (2010). On the relationships between lightning frequency and thundercloud parameters of regional precipitation systems. *Journal of Geophysical Research*, *115*, D12203. https://doi.org/10.1029/2009JD013385

Yair, Y., Shalev, S., Erlich, Z., Agrachov, A., & Katz, E. (2014). Lightning flash multiplicity in eastern Mediterranean thunderstorms. *Natural Hazards and Earth System Sciences*, *14*(2), 165–173. https://doi.org/10.5194/nhess-14-165-2014

Zhang, D., Cummins, K., Bitzer, P., & Koshak, W. (2018). A detailed look at the performance characteristics of the Lightning Imaging Sensor. In *Int. Lightning Detection Conf.,* 2018. Ft. Lauderdale, FL: Vaisala.